Modeling of a 3-D Light-Weight Space Manipulator

Hiroshi Ueno[1]
Yangsheng Xu

CMU-RI-TR-91-08

The Robotics Institute
Carnegie Mellon University
Pittsburgh, Pennsylvania 15213

April 1991

1. Visiting scientist from Shimizu Corporation in Japan.

Contents

List of Figures

List of Tables

Abstract

This report addresses the problem of modeling a 3-D flexible robot. First, the flexibility of each link is modeled by a lumped system assuming the bending deflection is not too large compared to the length of the link. Then the kinematics of a serial-chain flexible mechanism is obtained by using transform of rigid coordinates and flexible coordinates. The flexible coordinates frame is defined to represent deflections of each link. Based on the kinematics, overall dynamics is derived by Lagrangian method. To obtain transfer functions from the joint torque to the tip displacements, the inertial matrix must be invertible. We defined a set of new variables by which the inertial matrix is invertible. This provides a general approach for modeling a large class of multi-joint flexible robot, and the resultant model is simple to be implemented in real-time model-based control. Vibration experiments have been performed on the laboratory 3-D flexible model, and the experimental results have been compared to the analytical results.

Modeling of a 3-D Light-Weight Space Manipulator

1. Introduction

Considerable attention has been directed to the use of light-weight manipulators which provide an energy-efficient motion. Light-weight manipulators are especially feasible for applications in space, such as in orbit or on other planets, because the cost for launching is proportional to the weight of the object to be launched.

Many researchers have been investigating the problems of the light-weight manipulators with a substantial flexibility. Flexible mechanical chains have been treated as distributed mass system which results in a complex model and is difficult to control based on such a model. Most papers are limited to report on planar models with two or less degrees of freedom (DOF)[1,2]. On the other hand, most light-weight manipulators with a substantial flexibility can be modeled so that most of the mass is considered to be concentrated at joints or end-effectors, neglecting link weight[3]. In this way, modeling and control can be much simplified, and motion analysis of a 3-D flexible robot is possible.

In this paper, modeling of a multiple joints light-weight manipulator with a serial mechanical chain is discussed. This method is based on a lumped model from which linearized dynamics equations are derived. The 3-D manipulator that we have developed in the Robotics Institute of Carnegie Mellon University is composed of two light-weight links from the base to the end-effector[4,5]. By using the proposed method, the flexible space manipulator is modeled as an example. The method proposed can be used for modeling any multiple joint 3-D light-weight manipulator as long as the configuration is serial chain and link mass is negligible.

2. Modeling Strategy

The purpose of modeling is to obtain dynamics motion equations for the 3-D flexible manipulator. Since the tasks for the flexible manipulator in space require a large motion within its workspace, which presents a significant effect on the dynamics of the system, we would like to have a model in which considers a large 3-D motion is allowed. The degree of complexity of the model depends upon the required precision of the system in operation. The model derived in this report is feasible in terms of compromising between the necessary precision and the resultant complexity. This model is useful in the design of the mechanical configuration of a flexible robot, as well as the design of the manipulator controllers.

The manipulator considered consists of multiple rigid joints with actuators and high gear ratio drive trains, multiple light-weight links and an end-effector at the end. These compo-

nents are connected from the base ground to the end-effector in a serial configuration. Most flexible robots can be described in this way.

The following assumptions are made to obtain a linear model of the flexible robot. First, the mass of the light-weight links is neglected, compared to the mass of the joints. Second, we only consider the light-weight link shaped as a tubular or cylindrical slender beam which has the high tensile and shear stiffness. Therefore, the compliance of the link is considered in the bending and torsional directions, while the compliance in the other directions is neglected. Third, the deflections of the light-weight link is small with respect to the length of the link so as to obtain a linear model. Fourth, light-weight link is assumed to be connected to the center of the motor shaft so that the size of the joints is negligible. Fifth, the end-effector is assumed to be rigid. Sixth, gravity is not taken into account for space applications. We may include the gravity term in the model if needed.

We define joint mass, link stiffness in and around each axis of the Coordinates frame, and consider the joint positions and deflections as state-space variables. The kinematics of the manipulators is based upon the Coordinates transform between the two flexible links. The dynamics equation is derived using the Lagrangian method and linearization. When the variables are not independent, we propose to introduce new variables and modify the corresponding dynamics equations so that the system motion equation is not degraded by using a set of new variables. The eigenvalue analysis is performed based on the model. The method presents an effective way to compute a large class of 3-D flexible robots.

We use the following robot that has been developed in our lab as an example to illustrate the derivation procedure. This method can be applied to any manipulator for which the previous assumptions are valid.

The robot has a 2-DOF rigid rotary joint at the base and the tip respectively, a 1-DOF rotary rigid joint at the elbow, an end-effector at the tip, two light-weight links connecting the base to the elbow and the elbow to the tip as shown in figure 1. The lumped mass is concentrated at the elbow joint. The tip is assumed to be a lumped mass, although actually it stands for the two rigid joints and an end-effector of the robot developed in our laboratory.

3. Kinematics

The kinematics of the robot is derived in the following way. Physical properties, such as the mass and the length of the link are selected as the parameters. The variables to describe the state of the system are also defined. Two types of the Coordinates frames are then introduced; one is the rigid link coordinates frame located at the end of each link without the link deflection and the other is the flexible link coordinates frame located at the end with the deflection[6]. The coordinates transform between the rigid frame and the flexible frame are derived. The absolute tip position with respect to the base is formulated by using the coordinates transform.

Figure 1. Configuration of a Flexible Manipulator

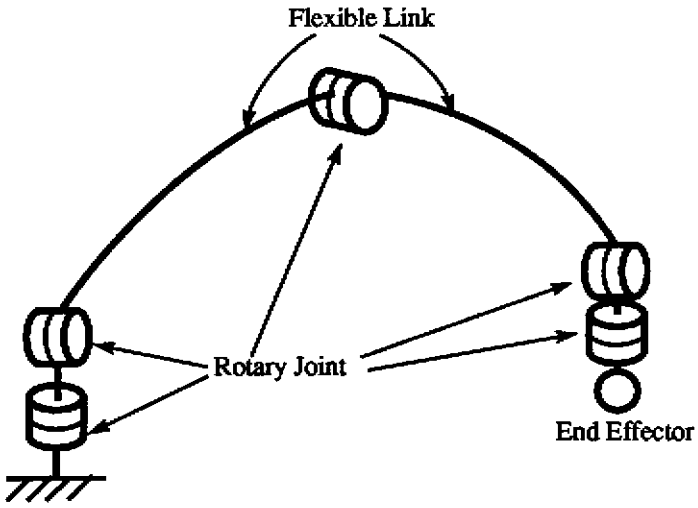

First, we consider the following parameters to describe the model of flexible robots. We denote the length of each links by l_i $(1 \leq i \leq 3)$, the mass of each joint by m_i, $(1 \leq i \leq 3)$, the inertia of each joint with the high gear ratio drive train by J_i $(1 \leq i \leq 3)$. The first link is rigid and for the second and third links, the bending stiffness, K_{bi}, and the torsional stiffness, K_{ti}, are considered. The inertia of the middle and the tip are neglected.

Second, we define the variables to describe the state of the motion as follows. The angle of each joint is denoted by θi $(1 \leq i \leq 3)$, the bending deflection in two axes at each link end is denoted by v_{yi}, v_{zi} (i = 2, 3), and the rotational deflection at each link end as ϕ_{xi}, ϕ_{yi}, ϕ_{zi} (i = 2, 3) are considered as the variables. It is noted that the variable for the torsional angular deflection of the third link, ϕ_{x3}, may be neglected, since no torsional torque is applied at the tip. However, it is still considered as one of the variables for the general description. The torque at each joint is denoted by τ_i $(1 \leq i \leq 3)$ is treated as a variable.

The position variables are referred to the generalized displacement, i.e., translational displacement and angular displacement. The force variables are referred to the generalized forces, i.e., torque and force. There are thirteen positions variables, three variables for the joint positions, ten for the deflection of the two links (five for each link). There are three force variables to describe joint torques. Other ten generalized forces are considered to be equal to zero. Figure 2 shows the parameters and the variables of the 3-joint flexible robot.

The Coordinates frame is defined at each link as shown in figure 3. The *i*th rigid coordinates frame is located at the end of the link *i* without deflection of the link *i*, while the *i*th flexible link coordinates frame is located at the end of the link *i* with deformation of the link *i*. To define the rigid coordinates frame, any of the available methods representing rigid robot kinematics, such as the D-H notation, can be used. To simplify the Coordinates transform, one of the axes must be parallel to the link *i* with no deflection. The *i*th flexible frame matches the *i*th rigid frame when the link *i* has no deflection.To distinguish the rigid coordinates frame from the flexible coordinates frame, prime *i*, *i*', is used for the *i*th rigid coordinates frame. The base coordinates frame is located at the base of the robot

Figure 2. Parameters and Variables of the Manipulator

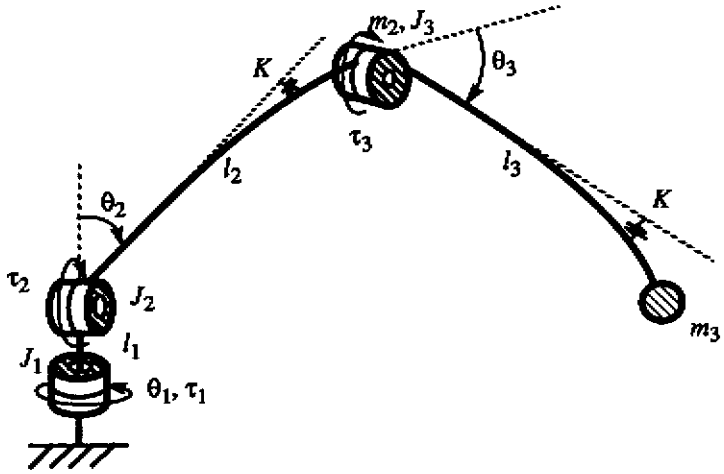

Parameters

l_i	$i = 1 \sim 3$	length of link i
m_i	$i = 2, 3$	mass of joint i
J_i	$i = 1 \sim 3$	joint inertia i with high gear ratio, ($J_i = n_i^2 J_{mi}$) n_i : gear ratio J_{mi} : motor inertia
K_{bi}	$i = 2, 3$	bending stiffness of link i, ($K_{bi} = \frac{E_i I_{bi}}{l_i^3}$) E_i : Young's modulus I_{bi} : moment of cross section area inertia
K_{ti}	$i = 2, 3$	torsional stiffness on link i, ($K_{ti} = \frac{G_i I_{ti}}{l_i}$) G_i : Shear modulus I_{ti} : polar moment of area inertia

Variables

θi	$i = 1 \sim 3$	angular displacement of joint i
v_{yi}, v_{zi}	$i = 2, 3$	bending deflection at the end of link i
ϕ_{xi}	$i = 2, 3$	torsional deflection of link i
ϕ_{yi}, ϕ_{zi}	$i = 2, 3$	angular bending deflection of link i
τ_i	$i = 1 \sim 3$	torque on joint i

Figure 3. Coordinates Frame

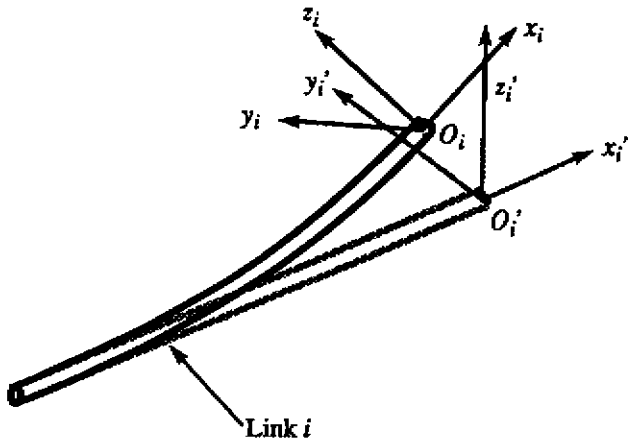

Figure 4. The Coordinates Frames of the Model

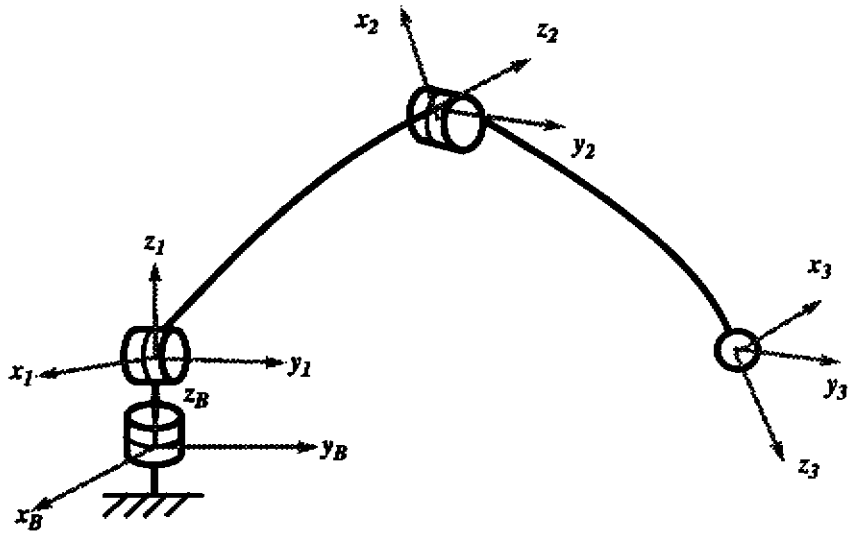

as the fixed reference. Figure 4 shows the coordinates frames of the model of the flexible robot discussed previously.

There are two types of Coordinates transform, the rigid coordinates transform and the flexible coordinates transform. The *i*th rigid coordinates transform changes the (*i-1*)th flexible coordinates frame into the *i*th rigid coordinates frame, while the *i*th flexible coordinates transform changes the *i*th rigid frame into the *i*th flexible frame. The *i*th rigid transform consists of the parameters and the variables related to the *i*th rigid link. The *i*th flexible transform consists of the variables related to the *i*th flexible link. The rigid transforms of the model shown in figure 4 can be defined as follows.

$$R_{1'}^{B} = \begin{bmatrix} \cos\theta_1 & -\sin\theta_1 & 0 & 0 \\ \sin\theta_1 & \cos\theta_1 & 0 & 0 \\ 0 & 0 & 1 & l_1 \\ 0 & 0 & 0 & 1 \end{bmatrix} \tag{1}$$

$$R_{2'}^{1} = \begin{bmatrix} \sin\theta_2 & 0 & -\cos\theta_2 & l_2\sin\theta_2 \\ 0 & 1 & 0 & 0 \\ \cos\theta_2 & 0 & \sin\theta_2 & l_2\cos\theta_2 \\ 0 & 0 & 0 & 1 \end{bmatrix} \tag{2}$$

$$R_{3'}^{2} = \begin{bmatrix} \cos\theta_3 & 0 & \sin\theta_3 & l_3\cos\theta_3 \\ 0 & 1 & 0 & 0 \\ -\sin\theta_3 & 0 & \cos\theta_3 & -l_3\sin\theta_3 \\ 0 & 0 & 0 & 1 \end{bmatrix} \tag{3}$$

The *i*th flexible transforms are defined as follows. The first flexible transform, $F_i^{i'}$, becomes unity, while $F_i^{i'}$, is defined as follows;

$$F_i^{i'} = \begin{bmatrix} 1 & -\phi_{z_i} & \phi_{y_i} & v_{x_i} \\ \phi_{z_i} & 1 & -\phi_{x_i} & v_{y_i} \\ -\phi_{y_i} & \phi_{x_i} & 1 & v_{z_i} \\ 0 & 0 & 0 & 1 \end{bmatrix} \tag{4}$$

The configuration of the robot with respect to the base coordinates frame is obtained by multiplication of these Coordinates transform matrices. The elbow position, X_2^B, and orientation, P_2^B, with respect to the base are,

$$X_2^B = \begin{bmatrix} x_2 & y_2 & z_2 & 1 \end{bmatrix}^T = R_1^B F_1^{1'} R_2^1 F_2^{2'} \begin{bmatrix} 0 & 0 & 0 & 1 \end{bmatrix}^T \tag{5}$$

$$P_2^B = \begin{bmatrix} 1 & 0 & 0 & 0 \\ 0 & 1 & 0 & 0 \\ 0 & 0 & 1 & 0 \end{bmatrix} R_1^B F_1^{1'} R_2^1 F_2^{2'} \begin{bmatrix} 1 & 0 & 0 \\ 0 & 1 & 0 \\ 0 & 0 & 1 \\ 0 & 0 & 0 \end{bmatrix} \tag{6}$$

The tip position, X_2^B, and orientation, P_2^B, with respect to the base frame, are, $i = 2,3$

$$X_3^B = \begin{bmatrix} x_3 & y_3 & z_3 & 1 \end{bmatrix}^t = R_1^B F_1^{1'} R_2^1 F_2^{2'} R_3^2 F_3^{3'} \begin{bmatrix} 0 & 0 & 0 & 1 \end{bmatrix}^t \tag{7}$$

$$P_3^B = \begin{bmatrix} 1 & 0 & 0 & 0 \\ 0 & 1 & 0 & 0 \\ 0 & 0 & 1 & 0 \end{bmatrix} R_1^B F_1^{1'} R_2^1 F_2^{2'} R_3^2 F_3^{3'} \begin{bmatrix} 1 & 0 & 0 \\ 0 & 1 & 0 \\ 0 & 0 & 1 \\ 0 & 0 & 0 \end{bmatrix} \tag{8}$$

These analytical formulations of the robot kinematics are needed in order to obtain the robot dynamics which is discussed in the next section.

4. Dynamics

In this section, we will derive the linearized relationship between the generalized displacement and the generalized force by using the parameters and the variables defined in the previous section. The dynamics of the model is obtained in the following manner. First, using the Lagrangian method, we derive the dynamics of the model. Second, the dynamics equations are linearized in terms of the variables by neglecting the centrifugal and Coriolis terms. The coefficient of each variable in the equations is assumed to be constant so that a time-invariant linear system is ensured. Third, the properties of the linearized dynamics system is discussed.

The Lagrangian principle is used to describe the system dynamics. In order to obtain the kinetic energy, we consider the joint inertia with the high gear ratio drive train as well as the mass at the elbow and the tip as follows:

$$T = \frac{1}{2}\left(\sum_{i=1}^{3} J_i \dot{\theta}_i^2\right) + \frac{1}{2}\left(\sum_{i=2}^{3} m_i (\dot{x}_i^2 + \dot{y}_i^2 + \dot{z}_i^2)\right) \tag{9}$$

The potential energy consists of the torsional strain energy and bending strain energy.

$$U = \sum_{i=2}^{3} \frac{1}{2} K_{ti} \phi_{xi}^2 + \left(\sum_{i=2}^{3} K_{bi} (3\upsilon_{yi}^2 - 3l_i \upsilon_{yi} \phi_{zi} + l_i^2 \phi_{zi}^2) \right) + \left(\sum_{i=2}^{3} K_{bi} (3\upsilon_{zi}^2 - 3l_i \upsilon_{zi} \phi_{yi} + l_i^2 \phi_{yi}^2) \right) \tag{10}$$

Based on the kinetic energy and potential energy, the Lagrangian equations are represented in the following form.

$$\frac{d}{dt}\left(\frac{\partial T}{\partial \dot{q}_i}\right) - \frac{\partial T}{\partial q_i} + \frac{\partial U}{\partial q_i} = f_i \tag{11}$$

The generalized displacement q_i and the generalized force f_i are defined as follows:

$$q = \left[q_1 \; q_i \; q_{13}\right] = \left[\theta_1 \; \theta_2 \; \upsilon_{y_2} \; \upsilon_{z_2} \; \phi_{x_2} \; \phi_{y_2} \; \phi_{z_2} \; \theta_3 \; \upsilon_{y_3} \; \upsilon_{z_3} \; \phi_{x_3} \; \phi_{y_3} \; \phi_{z_3}\right] \tag{12}$$

$$f = \left[f_1 \; f_i \; f_{13}\right] = \left[\tau_1 \; \tau_2 \; 0 \; 0 \; 0 \; 0 \; 0 \; \tau_3 \; 0 \; 0 \; 0 \; 0 \; 0\right] \tag{13}$$

The Lagrangian equation Eq(11) is nonlinear due to the second part of the kinetic energy, Eq(9). It is necessary to linearize the model so that we can obtain the natural frequencies of the model. The first term of Eq(11) can be divided into two parts; the first part can be linearized by the second derivative of the generalized displacement, $\ddot{q}_i$, and the second part which consists of the product of the first derivative of the generalized displacement, $\dot{q}_i$, is neglected. The second term of Eq(11) is negligible, since this term also consists of the product of the first derivative of the generalized displacement, $\dot{q}_i$. The product of the first derivative of the displacement forms the nonlinear centrifugal and Coriolis forces which are negligible under the assumption of not too rapid motion. The third term of Eq(11) is linearized by the generalized displacement, q_i. In this way, we get the linearized dynamic equation which only consists of the inertia and stiffness term as follows;

$$M\ddot{q} + Kq = f \tag{14}$$

$$M = \begin{bmatrix} M_{11} & 0 & M_{13} & 0 & M_{15} & 0 & M_{17} & 0 & M_{19} & 0 & 0 & 0 & 0 \\ 0 & M_{22} & 0 & M_{24} & 0 & M_{26} & 0 & M_{28} & 0 & M_{2a} & 0 & 0 & 0 \\ M_{13} & 0 & M_{33} & 0 & M_{35} & 0 & M_{37} & 0 & M_{39} & 0 & 0 & 0 & 0 \\ 0 & M_{24} & 0 & M_{44} & 0 & M_{46} & 0 & M_{48} & 0 & M_{4a} & 0 & 0 & 0 \\ M_{15} & 0 & M_{35} & 0 & M_{55} & 0 & M_{57} & 0 & M_{59} & 0 & 0 & 0 & 0 \\ 0 & M_{26} & 0 & M_{46} & 0 & M_{66} & 0 & M_{68} & 0 & M_{6a} & 0 & 0 & 0 \\ M_{17} & 0 & M_{37} & 0 & M_{57} & 0 & M_{77} & 0 & M_{79} & 0 & 0 & 0 & 0 \\ 0 & M_{28} & 0 & M_{48} & 0 & M_{68} & 0 & M_{88} & 0 & M_{8a} & 0 & 0 & 0 \\ M_{19} & 0 & M_{39} & 0 & M_{59} & 0 & M_{79} & 0 & M_{99} & 0 & 0 & 0 & 0 \\ 0 & M_{2a} & 0 & M_{4a} & 0 & M_{6a} & 0 & M_{8a} & 0 & M_{aa} & 0 & 0 & 0 \\ 0 & 0 & 0 & 0 & 0 & 0 & 0 & 0 & 0 & 0 & 0 & 0 & 0 \\ 0 & 0 & 0 & 0 & 0 & 0 & 0 & 0 & 0 & 0 & 0 & 0 & 0 \\ 0 & 0 & 0 & 0 & 0 & 0 & 0 & 0 & 0 & 0 & 0 & 0 & 0 \end{bmatrix} \tag{15}$$

$$M_{11} = J_1 + m_2 l_{2x}^2 + m_3 l_{23x}^2 \qquad M_{13} = m_2 l_{2x} + m_3 l_{23x} \qquad M_{15} = m_3 l_{23x} l_{3x}$$

$$M_{17} = m_3 l_{23x} l_{3z} \qquad M_{19} = m_3 l_{23x}$$

$$M_{22} = J_2 + m_2 l_2^2 + m_3 (l_2^2 + l_3^2 + 2 l_2 l_3 \cos\theta_3) \qquad M_{24} = m_2 l_2 + m_3 (l_2 + l_3 \cos\theta_3)$$

$$M_{26} = m_3 (l_3^2 + l_2 l_3 \cos\theta_3) \qquad M_{28} = m_3 (l_3^2 + l_2 l_3 \cos\theta_3) \qquad M_{2a} = m_3 (l_3 + l_2 \cos\theta_3)$$

$$M_{33} = m_2 + m_3 \qquad M_{35} = m_3 l_{3x} \qquad M_{37} = m_3 l_{3z}$$

$$M_{39} = m_3$$

$$M_{44} = m_2 + m_3 \qquad M_{46} = m_3 l_3 \cos\theta_3 \qquad M_{48} = m_3 l_3 \cos\theta_3$$

$$M_{4a} = m_3 \cos\theta_3$$

$$M_{55} = m_3 l_{3x}^2 \qquad M_{57} = m_3 l_{3x} l_{3z} \qquad M_{59} = m_3 l_{3x}$$

$$M_{66} = m_3 l_3^2 \qquad M_{68} = m_3 l_3^2 \qquad M_{6a} = m_3 l_3$$

$$M_{77} = m_3 l_{3z}^2 \qquad M_{79} = m_3 l_{3z}$$

$$M_{88} = J_3 + m_3 l_3^2 \qquad M_{8a} = m_3 l_3$$

$$M_{bb} = m_3$$

$$M_{aa} = m_3$$

$$l_{2x} = l_2 \sin\theta_2$$

$$l_{23x} = l_2 \sin\theta_2 + l_3 \sin(\theta_2 + \theta_3)$$

$$l_{3x} = l_3 \sin\theta_3$$

$$l_{3z} = l_3 \cos\theta_3$$

$$K = \begin{bmatrix}
0 & 0 & 0 & 0 & 0 & 0 & 0 & 0 & 0 & 0 & 0 & 0 & 0 \\
0 & 0 & 0 & 0 & 0 & 0 & 0 & 0 & 0 & 0 & 0 & 0 & 0 \\
0 & 0 & K_{33} & 0 & 0 & 0 & K_{37} & 0 & 0 & 0 & 0 & 0 & 0 \\
0 & 0 & 0 & K_{44} & 0 & K_{46} & 0 & 0 & 0 & 0 & 0 & 0 & 0 \\
0 & 0 & 0 & 0 & K_{55} & 0 & 0 & 0 & 0 & 0 & 0 & 0 & 0 \\
0 & 0 & 0 & K_{46} & 0 & K_{66} & 0 & 0 & 0 & 0 & 0 & 0 & 0 \\
0 & 0 & K_{37} & 0 & 0 & 0 & K_{77} & 0 & 0 & 0 & 0 & 0 & 0 \\
0 & 0 & 0 & 0 & 0 & 0 & 0 & 0 & 0 & 0 & 0 & 0 & 0 \\
0 & 0 & 0 & 0 & 0 & 0 & 0 & 0 & K_{99} & 0 & 0 & 0 & K_{9d} \\
0 & 0 & 0 & 0 & 0 & 0 & 0 & 0 & 0 & K_{aa} & 0 & K_{ac} & 0 \\
0 & 0 & 0 & 0 & 0 & 0 & 0 & 0 & 0 & 0 & K_{bb} & 0 & 0 \\
0 & 0 & 0 & 0 & 0 & 0 & 0 & 0 & 0 & K_{ac} & 0 & K_{cc} & 0 \\
0 & 0 & 0 & 0 & 0 & 0 & 0 & 0 & K_{9d} & 0 & 0 & 0 & K_{dd}
\end{bmatrix} \tag{16}$$

$$K_{33} = 12K_{b_2} \qquad K_{37} = -6l_2K_{b_2}$$

$$K_{44} = 12K_{b_2} \qquad K_{46} = -6l_2K_{b_2}$$

$$K_{66} = K_{t_2}$$

$$K_{77} = 4l_2^2K_{b_2}$$

$$K_{99} = 12K_{b_3} \qquad K_{9d} = -6l_3^2K_{b_3}$$

$$K_{aa} = 12K_{b_3} \qquad K_{ac} = -6l_3K_{b_3}$$

$$K_{bb} = K_{t_3}$$

$$K_{dd} = 4l_3^2K_{b_3}$$

Since the deflection is small, the inertia matrix, M, is not a function of the deflection variables. The dynamics equation obtained in the previous way has the following properties:

1. The inertia matrix, M, is symmetric.
2. The rigid arm inertia matrix can be extracted from the inertia matrix, M. The coefficients of M for the second derivative of the joint variables forms the rigid arm inertia matrix as follows:

$$M_R = \begin{bmatrix} M_{11} & M_{12} & M_{18} \\ M_{12} & M_{22} & M_{28} \\ M_{18} & M_{28} & M_{88} \end{bmatrix} \tag{17}$$

3. The stiffness matrix, K, comprises the two link stiffness matrices. The link stiffness matrix is a five by five symmetrical matrix, because of the reciprocal theorem under the assumption of small deflection. Moreover, the torsional stiffness on the x-axis is scalar decoupled. The bending stiffness along the y-axis and the z-axis is coupled to the angular bending stiffness on the z-axis and the y-axis, respectively. This property is the result of single cantilever.

4. The stiffness matrix, K, can be directly obtained from the link parameters. The following procedure can be used to derive the stiffness matrix, K. First, the coefficient of the stiffness matrix, K, for each joint variable is set to zero. Second, the known stiffness matrix for the single cantilever is substituted into each link stiffness matrix. Since each joint and stiffness matrix is decoupled from the others, the rest of the elements are set to zero.
5. The generalized force, τ, applies on the joint. No external force is considered in this case, and thus any deflection on the corresponding direction is zero.
6. The dynamics equation can be divided into two parts, one is for the tangential direction motion represented by θ_i, $v_{y2,3}$, $v_{x2,3}$, $\phi_{z2,3}$, while the other is for the radial direction motion which consists of θ_2, θ_3, $v_{z2,3}$, $\phi_{y2,3}$. This is understandable, since the axis of the first joint is perpendicular to the axes of the second and third joints regardless of the manipulator configuration.
7. Each variable may not be independent. This will be is discussed in the next section.

5. Variables Constraints

In the previous section, we obtained a linearized dynamics motion equation based on the Lagrangian method. In this section, we will obtain the natural frequencies of the model at the free mode where the generalized forces are zero. In order to derive the eigenvalues of the model we would like to obtain the generalized eigen-matrix, $M^{-1}K$, which is products of the inverse inertia matrix and the stiffness matrix. However, the inverse of M may not exist, since each generalized displacement may not be independent. The following is a procedure to obtain the natural frequencies of the model in the case of the existence of the variable dependency. This dependency can be observed physically as discussed below.

First of all, the angular torsional deflection of the third link, $\phi_{x3}(q_{11})$, may not occur, since a point mass is assumed at the tip. This implies that ϕ_{x3} may not be considered as a variable, since it is always zero. Therefore, the coefficient related to this variable should be simply deleted from the both inertia matrix, M, and the stiffness matrix, K. To be specific, the 11th row and column of both matrices are deleted.

Second, the angular deflection of the third link in the y-axis, $\phi_{y3}(q_{12})$, and the z-axis, $\phi_{z3}(q_{13})$, are dependent on the deflection at the end of the third link in the z-axis, $v_{z3}(q_{10})$, and the y-axis, $v_{y3}(q_9)$, respectively, because no moment of inertia exists at the center of the mass at the tip. This implies that the angular deflection of the third link can be replaced by the deflection on the third link. The 12th and 13th rows and columns are deleted in both inertia matrix and the stiffness matrix. The 9th and 10th diagonal elements are modified as follows:

$$K_{99}' = \frac{(K_{99}K_{dd} - K_{9d}^2)}{K_{dd}}$$
$$K_{aa}' = \frac{(K_{aa}K_{cc} - K_{ac}^2)}{K_{cc}} \qquad (18)$$

Third, the angular deflection of the second link in the y-axis, ϕ_{y2}, is dependent on the deflection of the third link in the z-axis, $v_{z3}(q_{10})$. $\phi_{y2}(q_6)$ is caused by the acceleration of the tip in z-axis, $\ddot{z}_3$. v_{z3} is also produced by $\ddot{z}_3$. Therefore the 6th variable and 10th variable are dependent.

$$(K_{46}\upsilon_{z_2}(q_4) + K_{66}\phi_{y_2}(q_6))\, l_3 = K_{aa}{}'\upsilon_{z_3}(q_{10}) \tag{19}$$

To be specific, a new variable, $v_{z3}{}'(q_{10}{}')$, is defined as the 10th variable and the 6th row and column are deleted in both M and K so that the two variables are combined into a new variable.

$$\upsilon_{z_3}{}'(q_{10}{}') \equiv (\upsilon_{z_3}(q_{10}) + l_3\phi_{y_2}(q_6)) \tag{20}$$

The new variable is defined in such a way that the 10th row and column elements of the inertia matrix, M, are the same as before. Using the new variable, we modify the 10th row and column of the stiffness matrix, K, as follows:

$$\begin{aligned} K_{44}'' &= \frac{(K_{44}K_{66} - K_{46}^2) + K_{44}K_{aa}{}'}{K_{66} + K_{aa}{}'} \\ K_{4a}'' &= \frac{K_{46}K_{aa}{}'\frac{1}{l_3}}{K_{66} + K_{aa}{}'} \\ K_{aa}'' &= \frac{K_{66}K_{aa}{}'\frac{1}{l_3}}{K_{66} + K_{aa}{}'} \end{aligned} \tag{21}$$

Forth, the angular deflection in the z-axis, $\phi_{z2}(q_7)$, and the torsional deflection, $\phi_{x2}(q_5)$, of the second link and the deflection for the y-axis of the third link, $\upsilon_{y3}(q_9)$, are dependent. ϕ_{z2} is caused by the acceleration of the tip in y-axis, $\ddot{y}$, so are ϕ_{x2} and υ_{y2}. Therefore, the 5th, 7th and 9th variables are dependent;

$$K_{55}\phi_{x2}(q_5)\frac{1}{l_3\sin\theta_3} = (K_{37}\upsilon_{y2}(q_3) + K_{77}\phi_{22}(q_7))\frac{1}{l_3\cos\theta_3} = K_{99}{}'\upsilon_{y3}(q_9) \tag{22}$$

A new variable, $\upsilon_{y3}{}'(q_9{}')$, is defined as 9th variable, and the 5th and the 7th row and column are deleted in both M and K so that the three variables are combined into the new variable.

$$\upsilon_{y3}{}'(q_9{}') \equiv \upsilon_{y3}(q_9) + l_3\sin\theta_3\phi_{x2}(q_5) + l_3\cos\theta_3\phi_{z2}(q_7) \tag{23}$$

The new variable is defined in such a way that the 9th row and column elements of the inertia matrix, M, are kept the same. Using the new variable, we modify the 9th row and column of and the stiffness matrix, K, as follows:

$$
\begin{aligned}
K_{99}'' &= \frac{K_{55}K_{77}K_{99}'}{K_{55}K_{77}+l_3^2\sin^2\theta_3K_{77}K_{99}'+l_3^2\cos^2\theta_3K_{55}K_{99}'} \\
K_{39}'' &= \frac{K_{55}K_{37}K_{99}'l_3\cos\theta_3}{K_{55}K_{77}+l_3^2\sin^2\theta_3K_{77}K_{99}'+l_3^2\cos^2\theta_3K_{55}K_{99}'} \\
K_{33}'' &= \frac{K_{55}(K_{33}K_{77}-K_{37}^2)+K_{99}'(K_{33}K_{77}-K_{37}^2)l_3^2\sin^2\theta_3+K_{33}K_{55}K_{99}'l_3^2\cos^2\theta_3}{K_{55}K_{77}+l_3^2\sin^2\theta_3K_{77}K_{99}'+l_3^2\cos^2\theta_3K_{55}K_{99}'}
\end{aligned}
\tag{24}
$$

Based on the four modifications above, a new inertia matrix is invertible. Moreover, we normalize the new inertia and stiffness matrices in order to facilitate the following procedures. The modified dynamic motion equations are as follows:

$$
\bar{M}\ddot{\bar{q}}'' + \bar{K}\bar{q} = \bar{\tau} \tag{25}
$$

$$
\bar{M} = \begin{bmatrix}
j_1+ml^2\sin^2\theta_2+l_x^2 & 0 & ml\sin\theta_2+l & 0 & 0 & l_x & 0 \\
0 & j_2+ml^2+l^2+1+2l\cos\theta_3 & 0 & ml+l+\cos\theta_3 & 1+l\cos\theta_3 & 0 & 1+l\cos\theta_3 \\
ml\sin\theta_2 & 0 & m+1 & 0 & 0 & 1 & 0 \\
0 & ml+l+\cos\theta_3 & 0 & m+1 & \cos\theta_3 & 0 & \cos\theta_3 \\
0 & 1+l\cos\theta_3 & 0 & \cos\theta_3 & 1+j_2 & 0 & 1 \\
l_x & 0 & 1 & 0 & 0 & 1 & 0 \\
0 & 1+l\cos\theta_3 & 0 & \cos\theta_3 & 1 & 0 & 1
\end{bmatrix} \tag{26}
$$

$$
\bar{K} = \begin{bmatrix}
0 & 0 & 0 & 0 & 0 & 0 & 0 \\
0 & 0 & 0 & 0 & 0 & 0 & 0 \\
0 & 0 & \bar{K}_{33} & 0 & 0 & \bar{K}_{36} & 0 \\
0 & 0 & 0 & \bar{K}_{44} & 0 & 0 & K_{47} \\
0 & 0 & 0 & 0 & 0 & 0 & 0 \\
0 & 0 & \bar{K}_{36} & 0 & 0 & \bar{K}_{66} & 0 \\
0 & 0 & 0 & \bar{K}_{47} & 0 & 0 & \bar{K}_{77}
\end{bmatrix} \tag{27}
$$

$$\bar{K}_{33} = \frac{3k\left(\frac{\cos^2\theta_3}{kl^2} + \frac{\sin^2\theta_3}{k_t} + \frac{1}{3}\right)}{\Delta 1}$$

$$\bar{K}_{36} = \frac{\frac{6\cos\theta_3}{4l}}{\Delta 1}$$

$$\bar{K}_{66} = \frac{1}{\Delta 1}$$

$$\bar{K}_{44} = \frac{12kl(kl+3)}{\Delta 2}$$

$$\bar{K}_{47} = \frac{-18kl}{\Delta 2}$$

$$\bar{K}_{77} = \frac{12kl^2}{\Delta 2}$$

$$\Delta 1 = \frac{\cos^2\theta_3}{4kl^2} + \frac{\sin^2\theta_3}{k_t} + \frac{1}{3}$$

$$\Delta 2 = 4kl^2 + 3 \tag{28}$$

$$\bar{q} = \left[\bar{\theta}_1\ \bar{\theta}_2\ \bar{v}_{y_2}\ \bar{v}_{z_2}\ \bar{\theta}_3\ \bar{v}_{y_3}\ \bar{v}_{z_3}\right] = \left[\theta_1\ \theta_2\ \frac{v_{y_2}}{l_3}\ \frac{v_{z_2}}{l_3}\ \theta_3\ \frac{v_{y_3}}{l_3}\ \frac{v_{z_3}}{l_3}\right]$$

$$\bar{\tau} = \left[\bar{\tau}_1\ \bar{\tau}_2\ 0\ 0\ \bar{\tau}_3\ 0\ 0\right] = \left[\frac{\tau_1}{K_{b_3}}\ \frac{\tau_2}{K_{b_3}}\ 0\ 0\ \frac{\tau_3}{K_{b_3}}\ 0\ 0\right] \tag{29}$$

$$j_i \equiv \frac{J_1}{m_3 l_3^2} \qquad m \equiv \frac{m_2}{m_3} \qquad l \equiv \frac{l_2}{l_3} \qquad l_x \equiv \frac{l_2}{l_3}\sin\theta_3 + \sin(\theta_2+\theta_3) = l\sin\theta_2 + \sin\theta_3$$

$$k \equiv \frac{K_{b_2}}{K_{b_3}} \qquad k_t \equiv \frac{K_{t_2}}{K_{b_3}} \qquad ' \equiv \frac{d}{d\omega} \qquad \omega \equiv \sqrt{\frac{K_{b_3}}{m_3 l_3^2}} \tag{30}$$

Eq(25) is the time-invariant linearized dynamic equation in terms of the robot configuration. We can obtain the natural frequencies of the model at each robot configuration in the following manner.

First, the configuration of the robot is determined by the joint. The inverse matrix of the new inertia is numerically obtained. Second, the inverse inertia matrix is multiplied by the stiffness matrix to obtain the eigen-matrix. Third, the eigenvalues of the eigen-matrix are computed and the natural frequencies of the system are square roots of the eigenvalues.

The natural frequencies can be used in the design of the robot controller and mechanical structure of the robot in order to consider the dynamics of the robot system.

6. Simulation and Experiment

The numerical simulation has been performed based on the model discussed above. The natural frequencies are obtained from the linearized dynamics equations. The inertia and

stiffness matrices in the dynamics equations are changed with the configuration of the flexible robot. In order to make the dynamics equation time-invariant, the small change in the configuration is assumed. The eigenvalues are analyzed at each configuration.

The parameters in Table 1 are used to formulate the dynamics equations. These parameters are calculated from components and parts of our experimental light-weight manipulator.

Table 1. Simulation Parameters

j_1	:	normalized joint 1 inertia (gear ratio 60:1)	0.01342
j_2	:	normalized joint 2 inertia (gear ratio 100:1)	0.03728
j_3	:	normalized joint 3 inertia (gear ratio 60:1)	0.01342
m	:	normalized mass 2	0.3846
ℓ	:	normalized length of link 2	1.000
k_t	:	normalized torsional stiffness on link 2	0.750
k	:	normalized bending stiffness on link2	1.000
ω	:	normalized time	7.631

Table 2 shows the simulation results of the natural frequencies. The configuration of the flexible robot is selected so that the tip moves along the plane $Z_B = 0$. The robot motion can be viewed as two types of motions, the tangential and radial motions. There are seven modes of vibrations at each configuration. The first three modes ($f = 0$) corresponds to the rigid mode. The lowest non-zero mode occurs in the tangential motion. For this mode, the frequency decreases as the angle of the third join increases. The second lowest non-zero mode is in the radial motion. In this mode, The frequency decreases slightly as the angle of the third joint increases.

Table 2. Simulated Natural Frequencies

θ_2 [deg]	90	60	45	30	15
θ_3 [deg]	0	60	90	120	150
mode 1 [rad/rad]	0.00(t)	0.00(t)	0.00(t)	0.00(t)	0.00(t)
mode 2 [rad/rad]	0.00(r)	0.00(r)	0.00(r)	0.00(r)	0.00(r)
mode 3 [rad/rad]	0.00(r)	0.00(r)	0.00(r)	0.00(r)	0.00(r)
mode 4 [rad/rad]	3.98(t)	2.79(t)	2.36(t)	2.14(t)	2.02(t)
mode 5 [rad/rad]	8.25(r)	8.25(r)	8.26(r)	8.30(r)	8.38(r)
mode 6 [rad/rad]	13.7(r)	12.7(r)	11.08(r)	10.0(r)	7.14(r)
mode 7 [rad/rad]	16.6(t)	13.3(t)	12.6(t)	12.5(t)	12.5(t)

t: tagential motion r: radial motion

The experiment has been performed to obtain the natural frequencies at certain configurations. The experimental robot has five DOF with a gripper as the end-effector as described in figure 1. The last two rigid joint and the griper can be considered to be concentrated at the tip as a lumped mass.

By sweeping the sinusoid torque from low to high frequency, the natural frequencies as the local peek of the sensors readings are measured. In order to verify the experimental natural frequencies of the tangential motion, we apply the torque to the first joint and measure the elbow and tip accelerations in the tangential direction, while locking the rest of joints. The comparison between the simulation and the experimental results are listed in Table 3. For the tangential motion, the analytical eigenvalue is slightly larger than that got from the experiments, because the parameters errors. However the ratio of the error is mostly the consistent to the others. Because of unmodel errors, such as the error in the tip inertia, the experiment has shown four modes of the vibration, while the simulation result has only three modes. The experiment the radial motion has not been performed.

Table 3. Experiment and Simulation of Natural Frequencies in Tangential Motion

θ_2 [deg]	56.27		111.82		77.64		90.0	
θ_3 [deg]	62.20		36.23		25.95		0.00	
	Experiment	Simulation	Experiment	Simulation	Experiment	Simulation	Experiment	Simulation
mode 1[rad/rad]	0.00	0.00	0.00	0.00	0.00	0.00	0.00	0.00
mode 2[rad/rad]	2.22(79.0%)	2.81	1.98(78.6%)	2.52	2.96(82.5%)	3.59	3.29(82.7%)	3.98
mode 3[rad/rad]	10.3(80.5%)	12.8	9.06(58.8%)	15.4	8.31(53.6%)	15.5	14.4(86.7%)	16.6
mode 4[rad/rad]	13.6	———	15.4	———	14.3	———	———	———

We have numerically obtained the transfer function of the linearized dynamic system. The transfer functions are defined as the seven generalized displacements with respect to the three generalized forces at each configuration. Because the tangential and radial motions can be decoupled to each other, we derive the transfer functions of each motion. Figure 5 and figure 6,7 show the transfer functions of the joint torques to the tangential and radial motions in Body-plot at a certain configuration, respectively. On the low frequency ranges, the gain of the joint variables has the second order slope, while the gain of the deflection variables has constants. This shows that the flexible model can be treated as the rigid model on the lower frequency range.

The experimental Body-plot in the tangential motion has been obtained at a certain configuration. The sinusoid torque on the first joint of the robot is applies as the input, while the elbow acceleration in the tangential directions are measured as the output. The elbow acceleration is selected so that the first mode of the vibration is visible. By measuring the magnitudes of the input and output at each frequency, the Body-plot of the elbow acceleration with respect to the first joint torque. is obtained as shown in figure 8. A sufficient large magnitude of the input torque is selected so that the stiction in the joint is not significant. The experimental results are similar to the simulation results.

Figure 5. Body Plot of Tangential Motion, θ_1/τ_1, v_{y2}/τ_1, v_{y3}/τ_1 ($\theta_2 = 60$ [deg],$\theta_3 = 60$ [deg])

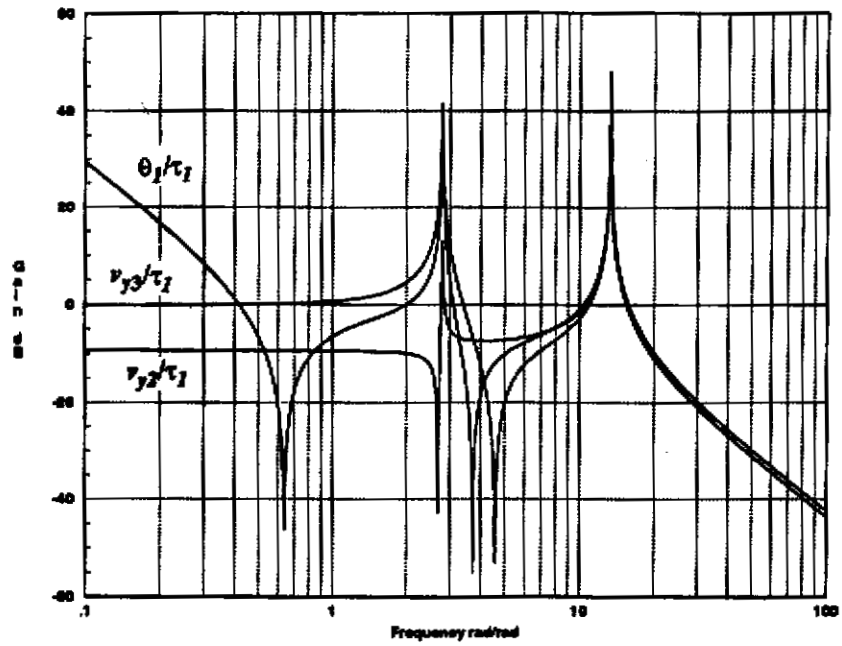

Figure 6. Body Plot of Radial Motion, θ_2/τ_2, θ_3/τ_2, v_{z2}/τ_2, v_{z3}/τ_2 ($\theta_2 = 60$ [deg],$\theta_3 = 60$ [deg])

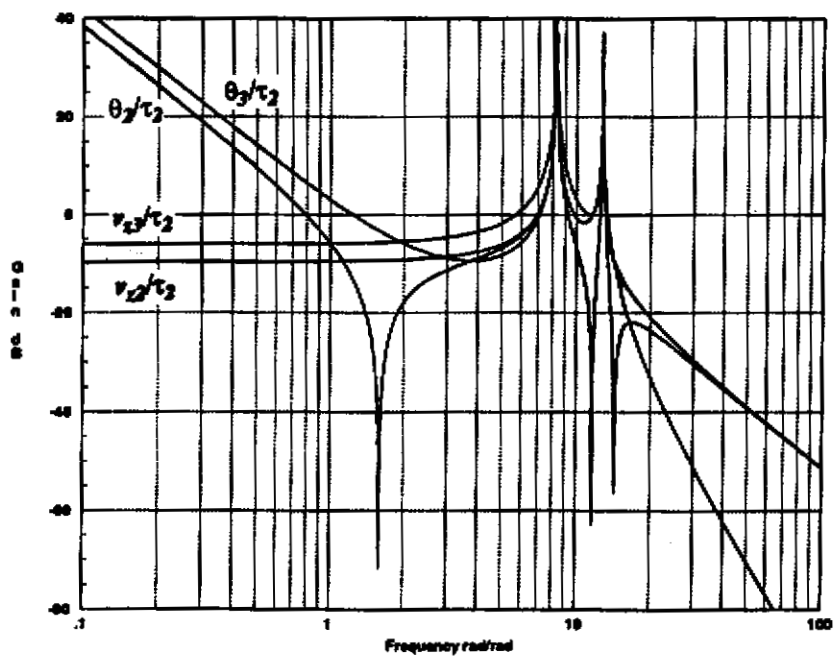

Figure 7. Body Plot of Radial Motion, θ_2/τ_3, $\theta 3/\tau_3$, v_{z2}/τ_3, v_{z3}/τ_3 ($\theta_2 = 60$ [deg], $\theta_3 = 60$ [deg])

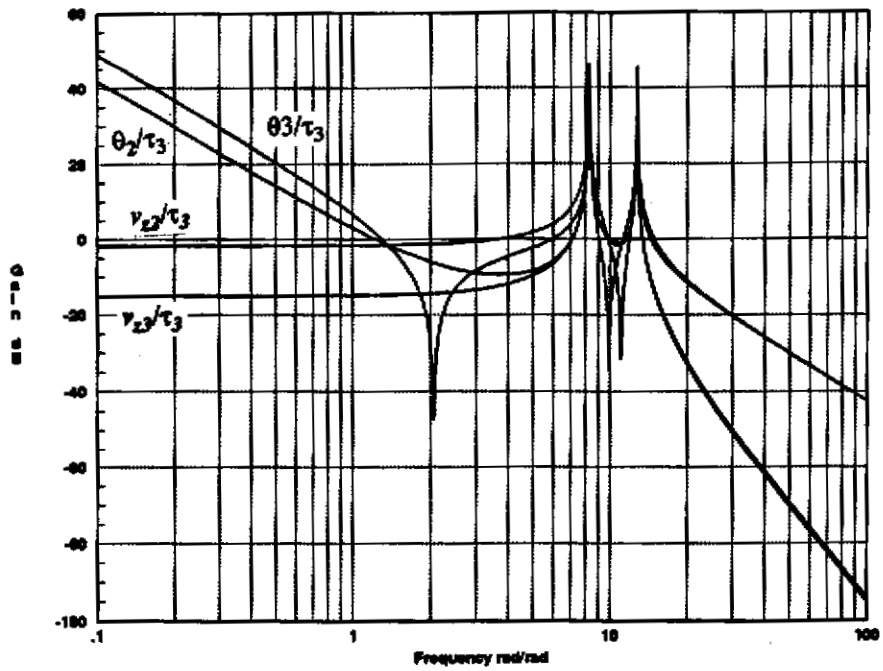

Figure 8. Body Plots of the elbow acceleration to the first joint, Experiment and Simulation

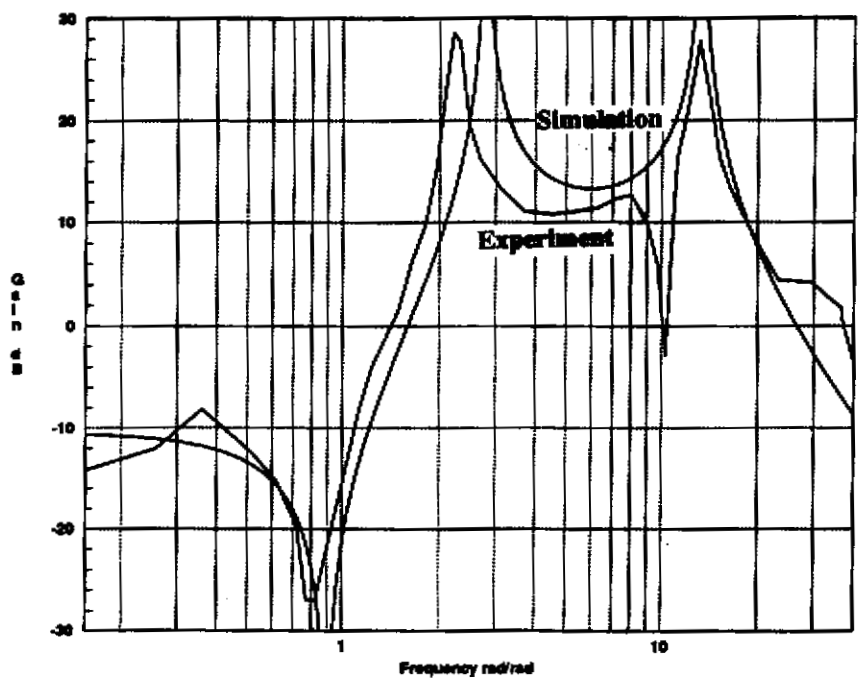

7. Conclusion

In this paper, a 3-D light-weight space manipulator is modeled. By concentrating the mass at the joint and neglecting the light-weight link mass, the model of the flexible robot can be linearized. The proposed method can also be used to model any arbitrary serial configuration flexible robot when the link mass is negligible. The method is simple and can be efficiency used in the real-time control, while it is of sufficient precision required for most of the light-weight manipulator for various cases are performed. The experimental result has verified the derived model.

References

[1] R. H. Cannon, and E. Schmitz, "Precise control of flexible manipulators", *Robotics Research,* 1985.

[2] F. Harashima, and T. Ueshiba. "Feedback control of a flexible manipulator with a parallel drive mechanism", *International Journal of Robotics Research,* Vol. 6, No. 4, 1987.

[3] Vicente Feliu, Kuldip S. Rattan and H. B. Brown, Jr., "A new approach to control single-link flexible arms", *The Robitics Institute Technical Report in Carnegie Mellon University,* CMU-RI-TR-89-8, 1989.

[4] H. Ueno, Y. Xu, H. B. Brown, Jr., M. Ueno, and T. Kanade, "On control and planning of a space station robot walker", *Proceedings of IEEE International System Engineering Conference,* 1990.

[5] H. B. Brown, Jr., M. Friedman, and T. Kanade, "Development of a 5-DOF walking robot for space station application", *Proceedings of IEEE International System Engineering Conference,* 1990.

[6] W.J. Book, "Analysis fo massless elastic chanins with servo controlled", *ASME Journal of Dynamic Systems, Measurements, and Control,* 1979.